β Actin and its mRNA Are Localized at the Plasma Membrane and the Regions of Moving Cytoplasm during the Cellular Response to Injury

Thomas C. Hoock, Patricia M. Newcomb, and Ira M. Herman

Program in Cell, Molecular and Developmental Biology, Tufts University Health Science Schools, Boston, Massachusetts 02111

Abstract. Previous work in our laboratory has shown that microvascular pericytes sort muscle and nonmuscle actin isoforms into discrete cytoplasmic domains (Herman, I. M., and P. A. D'Amore. 1985. *J. Cell Biol.* 101:43–52; DeNofrio, D., T. C. Hoock, and I. M. Herman. *J. Cell. Biol.* 109:191–202). Specifically, muscle (α-smooth) actin is present on the stress fibers while nonmuscle actins (β and γ) are located on stress fibers and in regions of moving cytoplasm (e.g., ruffles, lamellae). To determine the form and function of β actin in microvascular pericytes and endothelial cells recovering from injury, we prepared isoform-specific antibodies and cDNA probes for immuno-localization, Western and Northern blotting, as well as in situ hybridization. Anti-β actin IgG was prepared by adsorption and release of β actin–specific IgG from electrophoretically purified pericyte β actin bound to nitrocellulose paper. Anti-β actin IgGs prepared by this affinity selection procedure showed exclusive binding to β actin present in crude cell lysates containing all three actin isoforms. For controls, we localized β actin as a bright rim of staining beneath the erythrocyte plasma membrane. Anti-β actin IgG, absorbed with β actin bound to nitrocellulose, failed to stain erythrocytes. Simultaneous localization of β actin with the entire F-actin pool was performed on microvascular pericytes or endothelial cells and 3T3 fibroblasts recovering from injury using anti-β actin IgG in combination with fluorescent phalloidin. Results of these experiments revealed that pericyte β actin is localized beneath the plasma membrane in association with filopods, pseudopods, and fan lamellae. Additionally, we observed bright focal fluorescence within fan lamellae and in association with the ends of stress fibers that are preferentially associated with the ventral plasmalemma. Whereas fluorescent phalloidin staining along the stress fibers is continuous, anti-β actin IgG localization is discontinuous. When injured endothelial and 3T3 cells were stained through wound closure, we localized β actin only in motile cytoplasm at the wound edge. Staining disappeared as cells became quiescent upon monolayer restoration. Appearance of β actin at the wound edge correlated with a two- to threefold increase in steady-state levels of β actin mRNA, which rose within 15–60 min after injury and returned to noninjury levels during monolayer restoration. In situ hybridization revealed that transcripts encoding β actin were localized at the wound edge in association with the repositioned protein. Results of these experiments indicate that β actin and its encoded mRNA are polarized at the membrane–cytoskeletal interface within regions of moving cytoplasm.

E XPRESSION and sorting of contractile protein isoforms continues to be heavily studied in developing and differentiating systems (Bandman, 1985; Buckingham, 1985; Rubenstein; 1990; Schwartz and Rothblum, 1981). With respect to the development and remodeling of the blood vascular system (Noden, 1989), a number of reports have revealed the selective and timely expression of cytoskeletal and intermediate filament protein isoforms (Barja et al., 1986; Gabbiani et al., 1981, 1984; Owens et al., 1986; Rovner et al., 1986). Injury to the blood vessel wall induces the switching from a contractile to a synthetic phenotype; concomitantly, nonmuscle protein isoforms and the encoded mRNAs accumulate within vascular smooth muscle (Barja et al., 1986). During vessel repair, the non-muscle isoforms are replaced with their muscle counterparts (Gabbiani et al., 1984). In vitro modeling of the process reveals comparable phenotypic modulation as vascular smooth muscle cells grow and then become postconfluent in tissue culture (Chamley-Campbell et al., 1979; Barja et al., 1986; Owens et al., 1986).

Recent work has shown that microvascular pericytes, which have been dubbed the smooth muscle cell counterpart of the microcirculation, simultaneously express an abundance of muscle and nonmuscle contractile proteins in vitro and in vivo (DeNofrio et al., 1989; Herman and D'Amore, 1985; Herman, 1988; Herman and Jacobson, 1988; Herman et al., 1987; Joyce et al., 1985). Additionally, pericytes position these protein isoforms into distinct functional domains (DeNofrio et al., 1989). Muscle (α-smooth) actin is restricted to pericyte stress fibers whereas the nonmuscle ac-

tins (β and γ) are found on stress fibers and represent the only actins that can be extracted from motile cytoplasm (Herman and D'Amore 1985; DeNofrio et al., 1989). Simultaneous antibody localization studies on fibroblasts support the coexistence of the nonmuscle actins within this area (Otey et al., 1986). Another study using monoclonal antibodies and electron microscopy confirmed the preferential association of vascular smooth muscle actin within pericyte filament bundles present in microvessels perfused in situ (Skalli et al., 1989). In a related series of earlier experiments, isoform specific antibodies were used to reveal an association of γ actin with the mitochondria and costameres of skeletal muscle (Craig and Pardo, 1983; Pardo et al., 1983). Similarly, sorting of cytoplasmic myosins (Fallon and Nachmias, 1980; Gadasi and Korn, 1980; Joyce et al., 1985) and tropomyosins (Lin et al., 1988) has been suggested by antibody localization studies. These results suggest that specific contractile protein isoforms support unique cellular functions, but it is currently unknown how cells selectively position these proteins into specific subcellular compartments. With respect to microvascular pericytes, it is tempting to speculate that the regulation of microvascular permeability (Buchanan and Wagner, 1990; Herman and D'Amore, 1985; Herman and Jacobson, 1988), capillary contractility (Das et al., 1988; Kelley et al., 1987), or endothelial cell proliferation (Antonelli-Orlidge et al., 1989; Herman et al., 1987; Orlidge and D'Amore, 1987) are, in some ways, causally influenced by cytoskeletal composition. Furthermore, because of the intimate associations between endothelial cells and pericytes in vivo, specific contractile protein isoforms may also participate in microvascular remodeling during development.

Because of the association of nonmuscle actins with moving cytoplasm and the membrane-associated cytoskeleton we wished to more carefully examine whether one or both of the nonmuscle actins were selectively localized in the cell cortex. To this end, we produced anti-β actin IgG and now report on its specificity and localization within erythroid and non-erythroid cells. Anti-β actin IgG is preferentially associated with the plasma membrane of erythrocytes and all other nonmuscle cells tested, including microvascular pericytes, endothelial cells and fibroblasts. In erythrocytes, β actin was solely localized in the cell cortex beneath the membrane. In pericytes, β actin was juxtaposed to the plasma membrane and localized on a subset of stress fibers. In endothelial cells and 3T3 fibroblasts, which display directed

locomotion in response to mechanical injury, anti-β actin IgG staining was restricted to the leading edge of motile cytoplasm, intimately associated with the plasma membrane. Northern blot analysis of endothelial cells recovering from injury revealed that the steady-state levels of the mRNA encoding β actin rose significantly as the cells began their migration after injury. In situ hybridization revealed that a portion of the β actin mRNA pool is positioned with the β actin-enriched front of advancing cytoplasm that borders the wound edge. This preferential localization of β actin within regions of moving cytoplasm and the membrane-associated cytoskeleton strongly suggest a functional role in its regulation of cell shape and actin-based motility.

Materials and Methods

Culture of Microvascular Pericytes, Endothelial Cells, and Fibroblasts

Microvascular pericytes and endothelial cells were isolated and cultured from bovine retinal capillary fragments as previously described (DeNofrio et al., 1989; Herman and D'Amore, 1985). 3T3 cells were obtained from the American Type Culture Collection (Rockville, MD) and cultured in Ham's F12/DMEM containing 5% calf serum.

Preparation, Electrophoresis, and Western Blotting of Pericyte Extracts in One-dimensional Isoelectric Focusing Slab Gels

Microvascular pericytes, which were cultured in DMEM containing 10% bovine calf serum, were washed twice with warm PBS. Cells were extracted for 10 min at room temperature in a lysis buffer containing 0.5% Triton-X 100, 40 mM Hepes (pH, 7.15), 50 mM Pipes (pH, 6.9), 75 mM NaCl, 1 mM MgCl$_2$, 0.5 mM EGTA, 0.1 mg/ml pepstatin, 0.1 mg/ml soybean trypsin inhibitor, and 0.5 mM PMSF as described previously (DeNofrio et al., 1989). After lyophilization, samples were solubilized in 8 M urea, 5% 2-mercaptoethanol, 2% NP-40, and 2% ampholines (1:4 mixture of pH 4-6:5-7; Ampholytes; Bio-Rad Laboratories, Richmond, CA) and then focused to their isoelectric point in urea-acrylamide gels containing 2% ampholines as previously described (DeNofrio et al., 1989). Immunoblotting with anti-β actin IgG was accomplished after isoelectric focusing gel electrophoresis by equilibration of the actin-containing extracts bound to nitrocellulose. Blotted bands of interest were digitized using scanning laser densitometry as described in DeNofrio et al. (1989).

Immunoadsorption of Affinity-purified IgG

Lyophilized extracts from fractionated pericytes were electrophoresed in urea-acrylamide gels containing 2% ampholines as described above. After isoelectric focusing, gels were stained with 0.04% Coomassie blue G-250 in 5% perchloric acid. The stained segment of the slab gel containing β actin was excised and the gel pieces destained with 25% isopropanol and 10% acetic acid until the band became invisible. Approximately 1 μg of actin from replicate gels was transferred to nitrocellulose (Western blotting, see above) after equilibration for 1 h in 0.375 M Tris-Cl, pH 8.8 with 5% β-mercaptoethanol and 0.3% SDS. Nitrocellulose papers with the purified actin were blocked for 3-4 h by incubation in 20 mM Tris-Cl, pH 7.0 containing 0.9% NaCl, 0.05% Tween-20, 1.5% bovine serum albumin, and 6% goat serum. After the blocking step, papers with bound protein were washed in 0.02 M Tris-Cl, pH 7.0, with 0.9% NaCl (TBS) with 0.05% Tween-20 and then incubated in 100 μg/ml affinity-purified anti-β actin IgG previously released from an erythrocyte β actin affinity column as previously described (Herman and D'Amore 1985; DeNofrio et al., 1989). Antibodies were released into 200 μl of 200 mM glycine, pH 2.8. IgGs were immediately neutralized using 50 μl 1.0 M phosphate buffer, pH 7.5. Affinity selected anti-β actin IgG were dialyzed against TBS before characterization by Western blotting and immunofluorescence microscopy.

Injury of Retinal Endothelial and 3T3 Monolayers

To study the motile response to injury, we injured resting confluent

Table I. Quantitative Analysis of β Actin in Microvascular Pericytes

Structure	Luminance*	Quantity‡
Plasma membrane	2.15	2.3×10^4
Membrane foci	1.32	1.7×10^4
Stress fiber foci	1.80	2.3×10^4
Membrane spikes	2.15	2.4×10^4

* Arbitrary units/μm^2 have been standardized using anti-actin IgG luminance, where a value of 1.0 equals the average immunofluorescence present in one erythrocyte ($n = 50$).
‡ Number average/μm^2 of β actin molecules present within each pericyte microdomain using human erythrocyte anti-beta actin IgG immunofluorescence and (Pinder and Gratzer, 1983) where 5×10^5 equals the average number of beta actin molecules present in one erythrocyte.

monolayers using either a fire-polished Pasteur pipet (for antibody localization and in situ hybridization studies) or a stainless steel rake, which uniformly swept out slightly >50% of the resting population plated into 15-cm dishes, leaving the remaining cells to recover from the mechanical injury (for Northern blot analyses, see below).

Staining Erythroid and Nonerythroid Cells with Anti-β Actin IgG

Human Blood Smears. Peripheral blood from a finger poke was smeared onto subbed slides and air dried. Slides with dried smears were dipped into dry-ice cold acetone for 20 s before PBS washing. For localization studies, affinity selected, anti-β actin IgG (10–30 μg/ml) or comparable concentrations of anti-actin IgG, depleted of β actin reactivity by absorption to β actin bound to nitrocellulose, were used. Following a 60 min room temperature incubation, slides with blood smears were washed and re-incubated for an additional 60 minutes with 50 μg/ml goat anti-rabbit IgG labeled with tetramethyl rhodamine (Cooper Biomedical, Malvern, PA). Washed slides were viewed using a Zeiss IM 35 inverted fluorescent microscope equipped with a Zeiss planapochromat oil immersion objective lens (NA 1.4).

Microvascular Pericytes, Endothelial Cells, and Fibroblasts. Cells plated onto glass coverslips were fixed in 4% paraformaldehyde and then lysed in a 0.1% Triton-X lysis buffer containing 40 mM Hepes, pH 7.15, 50 mM Pipes, pH 6.9, 75 mM NaCl, 1 mM MgCl$_2$, and 0.5 mM EGTA. The staining procedure is described above and reported previously (DeNofrio et al., 1989). For image analysis of erythroid and nonerythroid cells stained with anti-β actin IgG, we used an IBM-AT based imaging workstation. The IBM-AT is equipped with the necessary hardware (Imaging Technologies FG-100 A/D card; Image Pro, Media Cybernetics, Silver Springs, MD) and software support (OPTIMA, Bioscan Inc., Edmonds, CA) for performing line and threshold imaging. The OPTIMA library of subroutines allows for automatic integration of bands (areas) of interest, either by line or threshold imaging. For quantitation of erythrocytes luminance, threshold imaging and background subtractions were performed directly on specimens placed on the fluorescence microscope or by delivering an analogue signal to the IBM-AT via CCD input of fluorescence micrographs. Each method yielded comparable results. In a typical calibration series, the luminance (area × integrated grey value) of 50 cells that were stained with specific antibody was obtained as an arbitrary number, which could then be compared to specimens stained with control antibodies or with other regions of interest in nonerythroid cells. Arbitrary units of luminance could then be expressed per unit area of cytoplasm. The relative concentration of β actin present in non-erythroid cells can be approached optically since (*a*) the number average of actin molecules present in erythrocytes is known (Pinder and Gratzer, 1983), (*b*) because erythrocytes express only β actin, and (*c*) the average luminance of an individual erythrocyte from an average number of erythrocytes can be held as a constant. (Table I).

Northern Blot Analysis

To assess the steady state levels of actin mRNA encoding β actin, which were present in resting monolayers and those migrating after injury, we cultured endothelial cells in 15-cm dishes. Six separate experiments were conducted in duplicate and triplicate. Resulting cell lysates were obtained from uninjured cells and during a time course after injury to include 0, 5, 15, 30, 60, and 90 min, as well as later time points, to learn of the mRNAs present in monolayers whose wounds were restored via migration and eventually, proliferation. We used three to four 15-cm dishes of injured cells for each time point. The machining of the stainless steel rake is such that uniform cellular zones (8–10 cell diameters) and wound zones (400–600 μm) are created equally and appear concentrically arranged over the substrate. From the 10^7 cells present in the uninjured 15-cm plate (ascertained by Coulter counting of replicate plates), routinely 5 × 10^6 cells remained after injury. Total cellular RNA was purified by density gradient centrifugation of guanidinium thiocyanate extracts through 5.7 M CsCl cushions (Chirgwin et al., 1979; Maniatis et al., 1982). RNA was then phenol extracted and ethanol precipitated. RNAs from control and experimentally injured endothelial cells were electrophoresed alongside one another through 1% agarose-formaldehyde gels before transfer to nitrocellulose and filter baking for 1 h in a vacuum oven at 75°C. Filters with blotted RNAs were hybridized in a solution containing 4× SSC, 50 mM Sodium phosphate, pH 7.1, 5× Denhardt's, and 10% Dextran sulfate at 65°C according to McHugh and Lessard (1988) using a nick-translated probe from a plasmid containing a 404-bp fragment encoding the 3'UT of β actin from bp 133–537, which was

prepared in the lab using standard procedures (Maniatis et al., 1982). The clone, which contained the fragment of the gene encoding human cytoplasmic beta actin, pHFb-3'UT-HF, was a generous gift of Drs. Kirk McHugh and Jim Lessard. Bands present on x-ray films exposed for identical time periods reflecting filters with identical amounts of RNA loaded (as previously determined by densitometry of ethidium bromide stained 28S and 18S RNAs present) were digitized using an LKB Scanning Laser Densitometer (LKB Instruments Inc., Gaithersburg, MD) as previously described (DeNofrio et al., 1989).

Localization of Actin mRNA by In Situ Hybridization

To localize actin mRNA in endothelial cells recovering from injury in vitro, we performed in situ hybridization using protocols adapted from previously published procedures (Maniatis et al., 1982; Lawrence and Singer, 1986; Warembourg et al., 1986). In essence, endothelial cells were plated onto 8-well culture chamber slides (Tissue Tek) at a confluent density as previously described (Herman and Castellot, 1987; Yost and Herman, 1990). Cells were injured using a fire polished Pasteur pipet before allowing the cells to recover after injury over a defined time course. Cells were fixed with 4% formaldehyde and were ethanol precipitated using a 95% solution prepared with RNase free water previously treated with DEPC in glassware that was baked. For in situ hybridization, 8 × 10^5 cpm in 200 μl hybridization buffer of ^{32}P-dCTP-labeled actin cDNA (see above), which was prepared by nick translation (10^8 cpm/μg DNA), was added to the chamber slide that was prehybridized for 2 h. After a 4-h incubation at 37°C, specimens were treated for 1 h at 37°C with 90 U/ml S1 nuclease in 30 mM sodium acetate, 3 mM zinc sulfate, 300 mM NaCl, with 5% glycerol, and 5 μg/ml salmon sperm DNA at pH 4.5. This step is critical for obtaining high signal-to-noise ratios since the S1 nuclease digests all single stranded, labeled DNA that was not hybridized to mRNAs present in the cells (Warembourg et al., 1986). Control groups were (*a*) treated with 0.01 mg/ml RNase A for 60 min at 37°C before specific cDNA incubation, (*b*) incubated with labeled plasmid DNA alone, or (*c*) untreated. Duplicate specimens from the experimental and control groups were washed with 0.5× SSC with 0.1% SDS at room temperature before dehydration through a graded series of ethanol, air drying, and then dipping in total darkness into a 1:1 dilution of NTB-2 (Nuclear Tracking Buffer; Eastman Kodak, Rochester, NY). Dipped slides were allowed to air dry in darkness before sealing into boxes with dessicant and storage at 4°C for 2–3 wk. Photographic emulsion dried onto slides with endothelial cells containing hybridized cDNAs were developed by dipping for 5 min into a 50% solution of D-19 developer cooled to 20°C. Slides were then sequentially dipped into a stop bath and fixer bath, respectively before water rinsing, air drying, and coverslipping. Slides with attached cells were viewed using either phase contrast or dark field optics. Exposed Tri-X negative films were developed in Acufine developer (Acufine, Inc., Chicago, IL) as described for fluorescence imaging.

Results

Affinity Isolation of β Actin–Specific IgG

We devised a procedure to prepare a polyclonal antibody specific for β actin using a two-step affinity selection procedure. Affinity-purified antibodies, which were previously shown to bind exclusively to the nonmuscle actin isoforms, were used. This affinity-purified preparation of anti–nonmuscle-specific IgG selectively binds to β and γ actins and contrasts the binding affinity of the unfractionated polyclonal anti-actin antibodies, which binds to all actin isoforms present in these crude cell extracts (Fig. 1, lanes *1* and *2*). When the affinity-purified anti–nonmuscle actin IgG is mixed with human erythrocyte actin covalently bound to Sepharose 4B, the mixture washed free of unbound IgG, and then subjected to an abrupt lowering of the pH, an IgG pool can be released. Western blot analysis and scanning laser densitometry reveals that the anti–actin IgG released from the β actin affinity column has 2.5 times the β actin cross-reactivity as compared to the starting IgG pool (Fig. 1, lane *3*). Such comparisons of IgG subfraction binding to actins were made on iden-
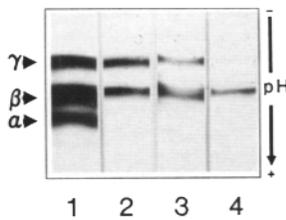
Figure 1. Affinity selection of anti–β actin IgG. Western blot analysis of pericyte extracts electrophoresed in a urea-acrylamide gel containing 2% ampholines. Lane *1*, anti-total actin IgG. Lane *2*, anti-nonmuscle actin IgG. Lane *3*, column-purified anti–β actin IgG. Lane *4*, affinity-selected anti–β actin IgG.

tical samples prepared from detergent-lysed cells that were electrophoresed and blotted to the same filters. The releasate from the β actin affinity column was then incubated with purified isoforms of actin electrophoretically transferred to nitrocellulose. Typically, 30–100 μg/ml anti–β actin was incubated with microgram amounts of electrophoretically purified β actin. After the absorption and subsequent washing steps, the nitrocellulose filters with bound IgG were treated transiently with 0.2 M glycine, pH 2.8 to release the bound antibody. The anti-actin IgG released from the nitrocellulose was determined to be >90% β actin specific, as judged by scanning laser densitometry of antibody binding to actins present in crude cell lysates and electrophoresed in urea-acrylamide isofocusing gels (cf. Fig. 1, lanes 2 and 3 with lane 4).

Localization of β Actin in Human Blood Smears

Smears of peripheral blood that were prepared and fixed to microscope slides were treated with two different preparations of anti-actin IgG: the β actin–specific IgG (Fig. 1, lane 4) and the β actin column-purified antibody (Fig. 1, lane 3), which was subsequently depleted of β actin–binding activity by absorption to β actin bound to nitrocellulose. As can be seen in Fig. 2 *A*, the anti–β actin IgG can be localized in all cells present in the peripheral blood, including erythrocytes (Fig. 2 *A*, arrow), platelets (Fig. 2 *A*, arrowhead), and white blood cells (not shown). Whereas the staining of the blood platelets with this affinity-purified IgG is extremely bright, the fluorescent images do not reveal any discrete subcellular localization patterns. This uniformly bright pattern of platelet fluorescence differs markedly from the anti–β actin IgG staining of erythrocytes (Fig. 2 *A*, arrow). In all cases, the anti–β actin-stained erythrocytes display a bright cortical ring of fluorescence, which completely circumscribes each cell. Anti–β actin IgG that was purified solely on β actin columns, which was subsequently absorbed with β actin, failed to stain the erythrocytes, but the staining of platelets (Fig. 2 *B*, arrowheads) and white blood cells (e.g., monocytes, Fig. 2 *B*, asterisk) was unaffected. Unlike the erythrocytes, which only express the β actin isoform, the white blood cells produce an abundance of each nonmuscle actin isoform.

β Actin Is Associated with the Plasma Membrane in Microvascular Pericytes

Whereas the nonmuscle specific (β and γ) actin antibodies localized these isoforms on stress fibers and within moving cytoplasm (DeNofrio et al., 1989; Herman and D'Amore 1985), we did not know, a priori, that the anti–β actin IgG staining of pericytes would be subtly different from the anti-

body pool from which it was initially derived. To assess these potential similarities and differences, we chose to simultaneously localize β actin with respect to the entire filamentous actin pool. Because we did not know whether the "generic" nonmuscle actin-specific IgG would compete for shared epitopes on the nonmuscle actin binding sites or whether it would sterically interfere with β actin IgG binding to cellular β actin, we used fluorescent phalloidin for colocalization experiments (Figs. 3 and 4).

When microvascular pericytes, which are incubated with β actin–specific IgG followed by reaction with NBD-phallacidin, are observed by fluorescence microscopy there is a unique β actin IgG staining pattern that is readily observed. The brightest β actin staining is found in association with the membrane-associated cytoskeleton, irrespective of whether the β actin IgG was purified solely by β actin column affinity or via the selection of β actin IgG by nitrocellulose adsorption (Fig. 3, *A* and *C* and Fig. 4, *A*, *C*, and *E*). Whereas the texture and overall localization patterns of these two antibody preparations were identical, the anti–β actin antibody staining of pericytes was brighter when we used the β actin-specific antibodies that was prepared by sequential purifica-
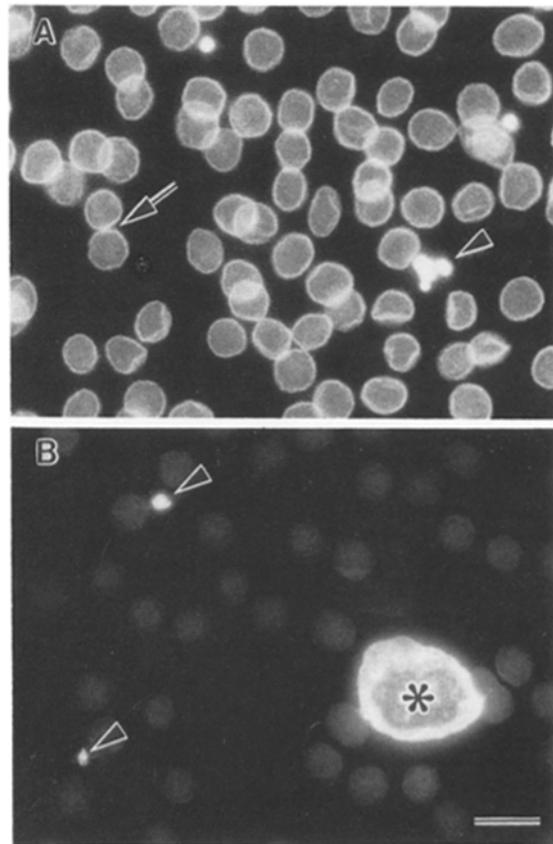

Figure 2. Localization of β actin in human peripheral blood smears. (*A*) Affinity-selected anti–β actin IgG. Note the localization of β actin at the erythrocyte plasma membrane (arrow) and the bright platelet staining (arrowhead). (*B*) Anti-actin IgG depleted of β actin reactivity by absorption. Note the loss of erythrocyte plasma membrane associated staining while the platelets (arrowheads) and leucocytes (monocyte shown [asterisk]) retain bright staining levels due to the presence of γ actin in these cells. Bar, 10 μm.
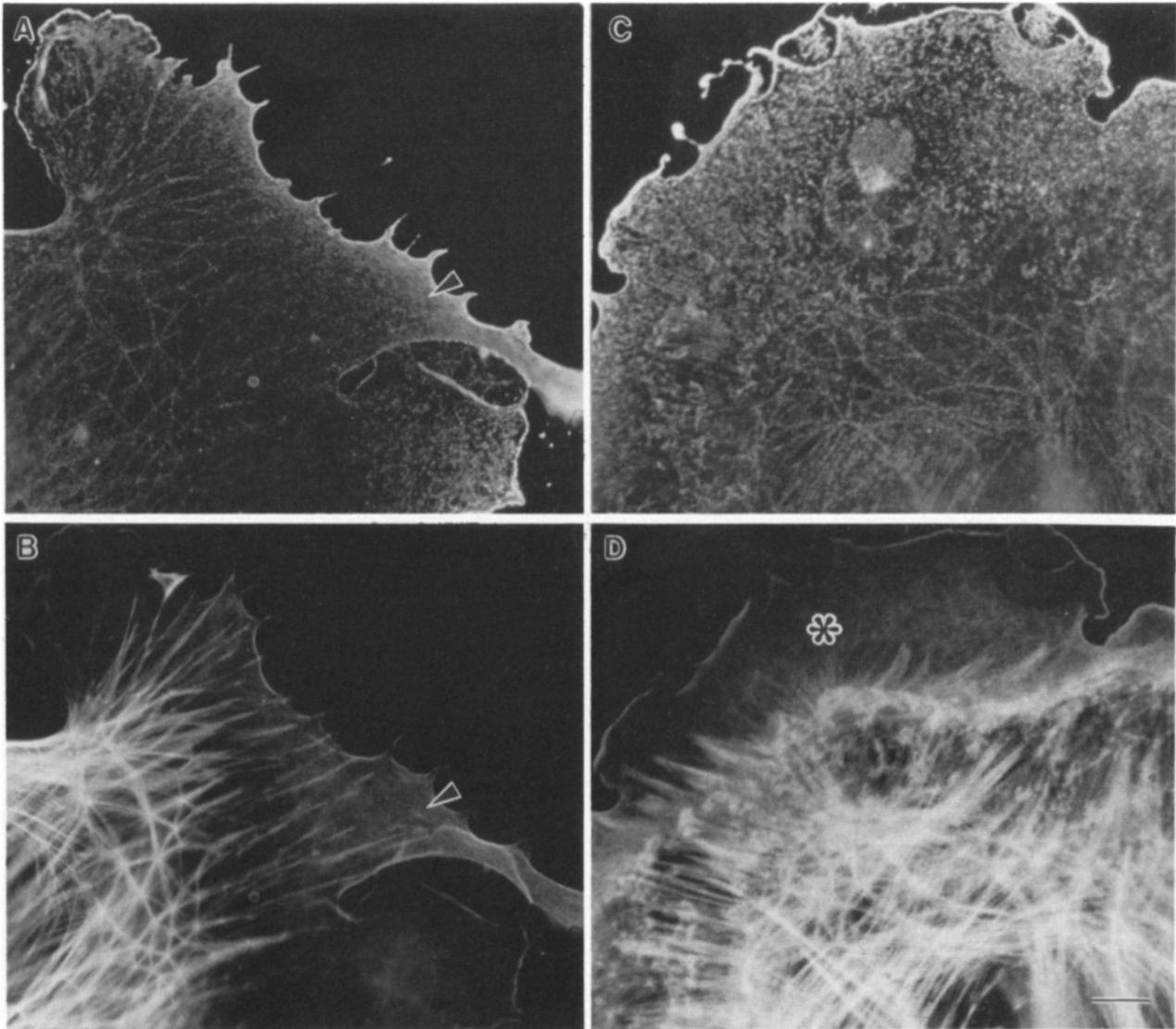
Figure 3. Simultaneous localization of pericyte actins using β actin-specific IgGs purified by Sepharose 4B–β actin chromatography and fluorescent phalloidin. (*A* and *C*) Anti–β actin IgG. (*B* and *D*) NBD-phallacidin. Note the cortical plasma membrane staining and bright focal fluorescence in *C*, also note the diffuse fluorescence adjacent to the membrane in *A*, and the absence of paralleled F-actin staining in *B* (arrowhead). Note the lack of punctate filamentous actin staining in the fan lamellae in *D* (*asterisk*). Bar, 10 μm.

tion (over β actin affinity columns followed by nitrocellulose adsorption). In addition to the bright rim of β actin fluorescence associated with the membrane, there are bright foci of anti–β actin IgG fluorescence present in fan lamellae and other motile structures. This contrasts the phalloidin staining patterns in these regions, which is uniformly amorphous (Fig. 3, *C* and *D* and Fig. 4, *C* and *D*, *asterisks*). By through focusing, we determined these β actin foci to be associated with the ventral plasma membrane. Ratio image analysis of the β actin and phalloidin-stained pericytes revealed that the anti–β actin IgG staining was 2–10 times brighter than the phalloidin staining in identical regions, i.e., membranes, pseudopods, etc. (Table I). By image analysis and comparison to the staining of erythrocytes we estimated the number average of β actin molecules present within each pericyte microdomain (Table I). Using a constant concentration of antibodies and identical reaction conditions, we determine

that the pericyte membrane–cytoskeletal interface contains at least twice the amount of β actin/μm² when compared to the human erythrocyte.

In addition to the bright rim of β actin fluorescence that is associated with the plasma membrane and the foci of β actin that are interspersed through the ventral portions of moving cytoplasm, we found stress fibers that contained domains enriched in β actin. Upon close inspection, the bright foci of β actin fluorescence in nonstress fiber containing regions closely resembled, in size and luminance, the bright spots of β actin staining associated with the ends of this stress fiber subset (Figs. 3 and 4). Strikingly, those stress fibers that were seen to directly end at the plasma membrane contained a localized concentration of anti–β actin IgG at the stress fiber ends where they abut the membrane (Fig. 4 *E, arrowhead*). Phalloidin staining in the identical cell and cells like those presented revealed a continuous, uninterrupted F-actin
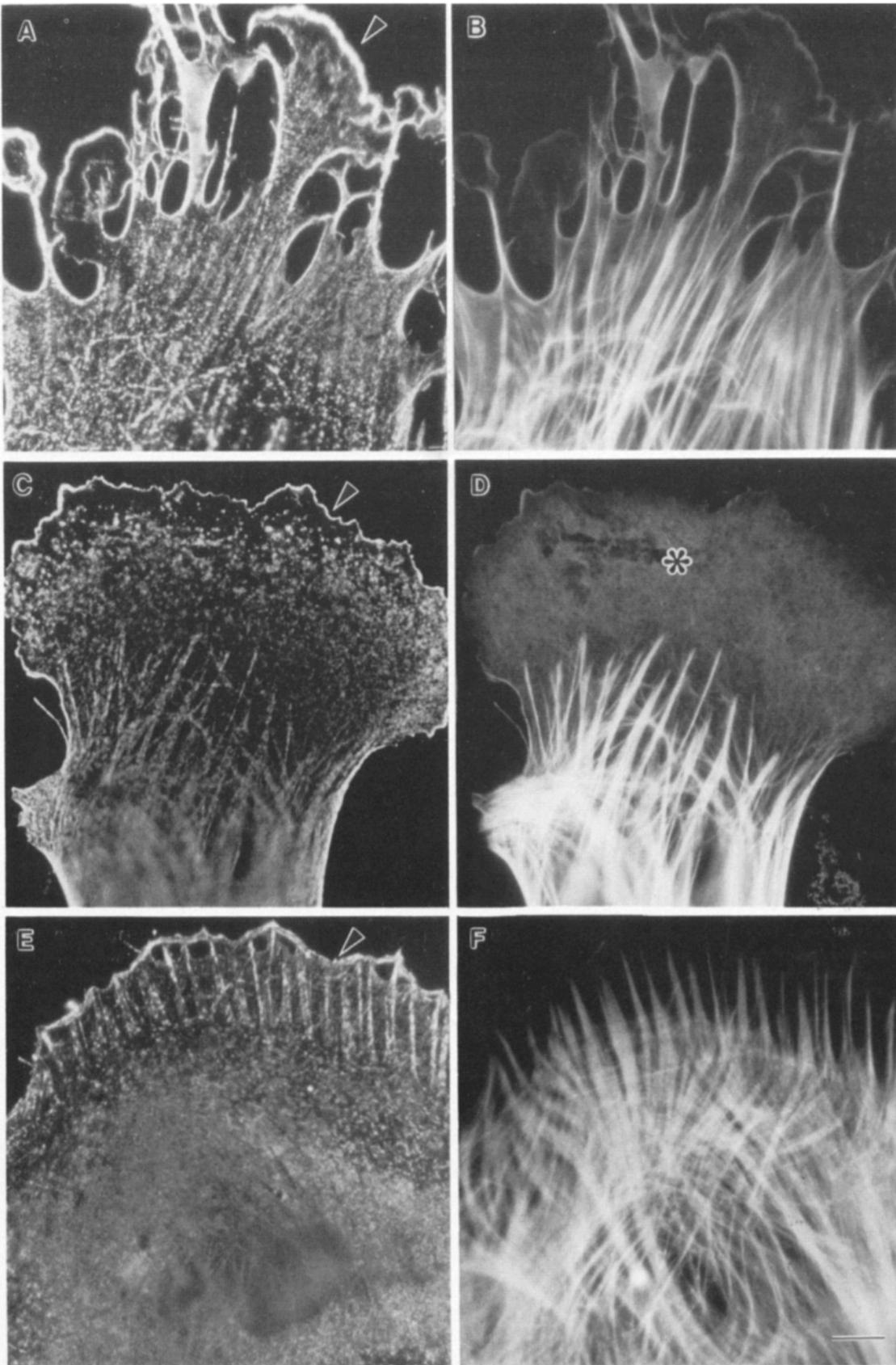
Figure 4. Pericyte β actin is localized at the membrane–cytoskeletal interface. (*A*, *C*, and *E*) Affinity-selected anti–β actin IgG. (*B*, *D*, and *F*) NBD-phallacidin. Note the bright fluorescence associated with cortical plasma membrane (*arrowheads*), and the focal fluorescence throughout the cells. Note the amorphous staining pattern in the large fan lamellae in *D* (*asterisk*). Bar, 10 μm.

staining pattern, which continues over the entire length and fills the entire "girth" of the stress fiber (Fig. 4 F). Additionally, there is another subclass of stress fibers that contain focal concentrations of anti-β actin fluorescence seemingly all along the length of these fibers. These stress fibers are apposed to the ventral plasma membrane and are running in parallel array to the plane of the membrane (Fig. 4, A and C). Stress fibers that do not ostensibly terminate in the plasma membrane and those that are not associated with the ventral plasma membrane cannot be localized with the anti-β actin IgG, but can be seen clearly with NBD-phallacidin (compare, e.g., the images shown in Figs. 3 and 4).

β Actin Is Localized at the Wound Edge in Endothelial Cell Monolayers Migrating after Injury In Vitro

Since the localization pattern for anti-β actin staining in microvascular pericytes suggested that this actin isoform was preferentially associated with regions of the cell that were actively motile, we injured resting monolayers of endothelial and 3T3 cells knowing that a directed migratory response would ensue after injury. In this way, we could specifically examine a population with a defined motile response and ask whether β actin was localized within the regions of moving cytoplasm. Two-dimensional gel and Western blot analysis of endothelial cell lysates indicate that β actin is a minor component of the actin cytoskeleton when compared on a weight basis with γ actin (1:6, Herman, I., unpublished observations). Interestingly, resting confluent monolayers of endothelial cells, which were simultaneously or sequentially stained with NBD-phallacidin, failed to revealed any detectable anti-β actin fluorescence. In some cases, bright anti-β actin IgG fluorescence was seen in association with pseudopods protruding underneath the resting monolayers. (Fig. 5 A, arrows). Whereas the phallacidin staining pattern revealed an abundance of stress fibers, stress fiber staining was not detectable with anti-β actin IgG (Fig. 5). Within 5 min after injury, we detected bright, membrane-associated anti-β actin fluorescence in the cytoplasm bordering the wound edge (Fig. 5 C, arrow). This staining was typically associated with ruffling membranes, pseudopods, and later with the veil of cytoplasm present within fan lamellae (Fig. 5). Endothelial cells continue to spread within the denuded zone over the next 60–90 min. Once the cells bordering either side of the narrow wounds begin to contact one another, anti-β actin IgG staining at the leading edge disappears. This occurs roughly 90–110 min after injury (Fig. 5). Simultaneous localization of filamentous actin with NBD-phallacidin reveals an abundance of actin in quiescent regions, which are unstained with anti-β actin IgG.

Northern Blot Analysis of the Endothelial Actin mRNA Response to Injury

Equal amounts of total RNAs from control (resting and confluent) monolayers and those recovering from mechanical injury were electrophoresed and blotted alongside one another onto the same nitrocellulose filters before hybridization with a 3'UT- β actin-specific cDNA probe, prepared in the lab according to McHugh and Lessard (1988). A typical Northern blot exposed during the endothelial response to injury reveals that the steady-state levels of β actin mRNA fall to 50% to the steady-state levels present in confluent

monolayers immediately following injury (Fig. 6, lane 1 and 2). Results of these experiments revealed that the actin mRNA levels rise from 2 to 4.5-fold from 0 time through 15 min after injury and continue to rise up to 90 min after injury, after which time endothelial actin mRNA levels return to their preinjury levels present in confluent cultures (Fig. 6).

## Localization of Actin mRNA in Wounded Endothelial Monolayers

Since Northern blot analysis indicated that the β actin mRNA levels rose from barely detectable levels immediately after injury to several times those steady-state levels within cells migrating 15 min after injury, we wished to examine whether the cytoskeleton partitioned a network of mRNA encoding β actin. Using our labeled cDNA probe for β actin, we treated fixed monolayers and permeabilized monolayers at specific times after injury. At 0 time there was no apparent localization of silver grains at the wound edge, except for occasional grains that were randomly scattered over the cells and coverglass. This pattern was comparable to monolayers that had been treated with labeled vector alone (pBR322) or monolayers that were treated with 100 μg/ml RNase before treatment with the specific actin cDNA probe (data not shown). Within 5 and up to 90 min after injury, phase-contrast (Fig. 7, A and B) and dark field optics (Fig. 7, C and D) revealed a nonrandom enhancement of silver grains over the veil of cytoplasm in some of the cells bordering the wound edge, particularly within pseudopods, filopodial extensions, and fan lamellae. Whilst the predominance of radio-labeled actin cDNA–endothelial actin mRNA hybridization was localized in the perinuclear region, the autoradiographic signal along the wound edge was significant when compared to the random hybridization seen over the wound zone and nuclear compartments.

Discussion

We used a two-step affinity selection procedure to prepare a polyclonal antibody that specifically binds to β actin. This anti-β actin IgG recognizes β actin, but not α or γ actins as judged by Western blots of crude cell lysates electrophoresed through isoelectric focusing gels. In addition, this antibody preparation was shown to be specifically associated with β actin in erythroid and all nonerythroid cells tested (vascular endothelial cells, microvascular pericytes and 3T3 fibroblasts). Northern blot analysis and in situ hybridization confirmed and extended the antibody localization studies, indicating a temporal and spatial accumulation of mRNA encoding β actin coincident with the motile response to injury. This transient increase in the steady state levels of β actin mRNA coupled with the placement of these nascent mRNAs at the edge of wounds where directed migration occurs may allow cells to respond to injury in an efficient manner, perhaps by local translation of contractile proteins.

Isolation of Anti-β Actin IgG

In the past, we and others have been successful in obtaining isoform specific actin antibodies using affinity selection procedures (DeNofrio et al., 1989; Herman and D'Amore; 1985; Pardo et al., 1983) or procedures using peptides of
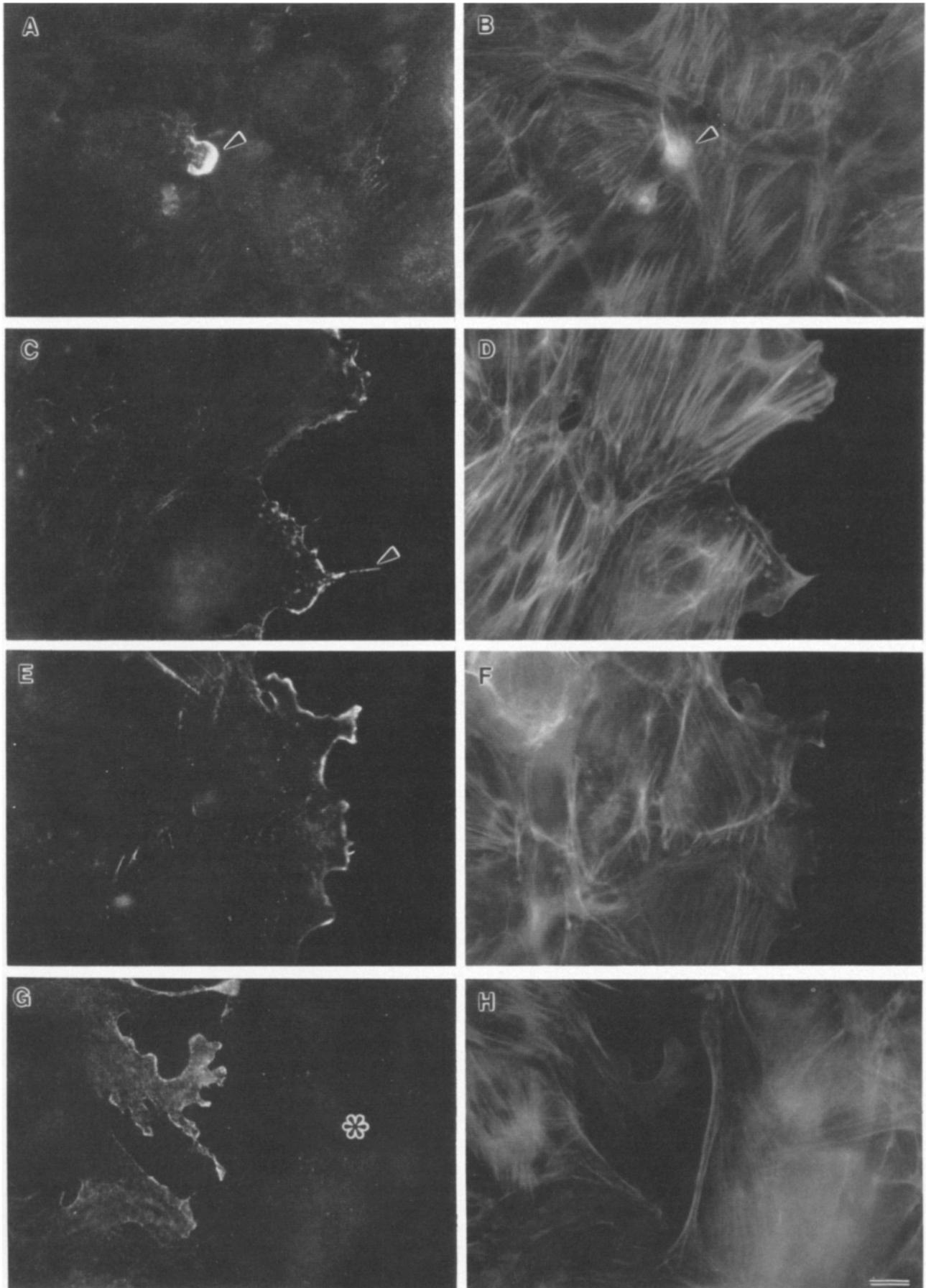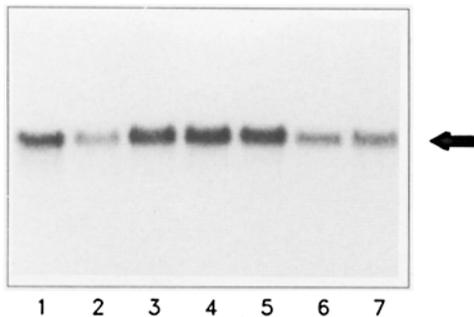
Figure 6. Endothelial cell actin mRNA response to injury. Northern blot analysis of total endothelial cell RNA was performed on equal amounts (10 μg) of RNA that was previously isolated from endothelial cells before injury (lane 1), immediately after injury, 0 time (lane 2) and subsequently 15 (lane 3), 30 (lane 4), 60 (lane 5), 90 min (lane 6), and 24 h after injury (lane 7). RNA electrophoresed and blotted onto nitrocellulose was hybridized with ^{32}P-dCTP actin cDNA specific for the 3'UT region of β actin mRNA. Arrow indicates 2.1 kb.

specific actin isoforms as immunogens (Otey et al., 1986). These affinity-purified antibodies have proven to be invaluable for biochemical and morphological studies aimed at revealing the relative amounts of particular contractile protein isoforms in specific cellular regions. Furthermore, there has been the suggestion, based on this technology and other experimental findings, that placement or sorting of cytoskeletal protein isoforms mediates specific cell functions, e.g., motility and controlling shape.

Using a modification of our early affinity selection strategies, we have succeeding in preparing an antibody that specifically binds to β actin. Purification of the nonmuscle (β/γ specific) actin antibodies on platelet actin columns (Herman and D'Amore, 1985) only yields a nonmuscle specific antibody. Furthermore, selection of anti-β actin IgG by passage of nonmuscle actin-specific IgG over β actin bound to Sepharose 4B does not completely remove IgG that are cross-reactive with γ actin. (Fig. 1, lane 3). This is apparent when peripheral blood smears are stained with this antibody preparation after its depletion of β actin reactivity. Under these experimental conditions, platelets and white blood cells stain, but erythrocytes do not. Image analysis of bands present in blots of crude cell lysates, which were reactivated with the column-purified anti-β actin IgG, reveal a 2.5-fold preference for β vs. γ actin (Fig. 1, lane 3 vs. lane 2). This could not be altered by increasing the molar ratio of anti-nonmuscle actin IgG to β actin bound to the column. However, increasing the molar ratio of IgG to actin from 1.5 to 3:1 does increase the yield of antibody released from the column by two to threefold. Further increasing the IgG/actin

molar ratio to 10-fold did not alter the recoverability or specificity of the antibodies obtained (Herman, I., unpublished data). We succeeded in preparing an antibody that was solely specific for β actin using electrophoretically purified β actin bound to nitrocellulose as a solid phase matrix to bind and release anti-β actin IgG (Fig. 1, lane 4). Similar procedures have been successfully used to isolate antibodies specific for other cytoskeletal elements (Olmsted, 1981). Nitrocellulose adsorption allowed only antibodies that possessed binding affinity for β actin to be recovered. It is unknown why binding of the antibodies to β actin bound to Sepharose 4B failed to yield the purified preparation of β actin-specific IgG that was recovered from the nitrocellulose paper. Perhaps the electrophoretic treatment of the β actin, itself, slightly altered the antigen in a way that prevented antibody recombination with shared epitopes on the two nonmuscle actin isoforms. Another advantage of this technology was that small volumes of immunoglobulin could be manipulated and the antibodies that were recovered were "well-behaved," based on (a) their ability to detect only β actin in a crude cell lysate (Fig. 1, lane 4) and (b) specific anti-β actin localization patterns that could be detected by immunofluorescence. Further, since these antibodies are polyclonal in origin, problems seen with monoclonal antibodies, i.e., species and tissue cross-reactivity, were not encountered. This may be of general interest when issues regarding developing systems are considered.

β Actin in Erythroid and Nonerythroid Cells

Work in the recent past has documented that erythrocytes from a number of species express only β actin (Bennett, 1985; Brenner and Korn, 1980; Cohen and Foley, 1982; Pinder and Gratzer, 1983; Tsukita et al., 1984). In addition to their unique expression of this single actin isoform, the cytoskeleton of erythrocytes contains an interesting β tubulin, one that allows for an enormously long microtubule (Murphy and Wallis, 1983; Murphy, 1988). While the similarities in actin and tubulin structure only extend, perhaps, to their residence within the cytoskeleton, the fact that a specific isoform of each multigene family is expressed in erythrocytes is noteworthy; especially in light of the erythrocytes unique shape and deformability. In other nonmuscle cells, isoelectric variants of the actin and tubulin gene families are coexpressed. Perhaps the unique biophysical and metabolic constraints placed upon the erythrocyte dictate this pathway for specialized cytoskeletal protein subsets.

Early work on erythrocyte actin indicated that, in vivo, erythrocyte actin filaments are ∼100 nm long (Atkinson et al., 1982; Pinder et al., 1977; Pinder and Gratzer, 1983; Tsukita et al., 1984). Actin filaments assembled in vitro from β actin present in erythrocyte ghosts are comparably

Figure 5. Endothelial cells position β actin at the leading edge during the migratory response to injury. (A, C, E, and G) Anti-β actin IgG. (B, D, F, and H) NBD-phallacidin. Note that in the uninjured population, the only anti-β actin fluorescence is localized at the tip of a pseudopod that has penetrated beneath the confluent monolayer (A, arrowhead). The total pool of filamentous (β + γ) actin can be seen in B. During the response to injury the appearance of β actin staining within pseudopods and fan lamellae occurs rapidly. C and D = 10 min postinjury; E and F = 60 min; G and H = 120 min. Note that the bright staining of anti-β actin IgG persists until cells stop migrating when they contact each other from either side of the wound edge (asterisk, G). The intensity and distribution of NBD-phallacidin staining is unchanged during the motile response to injury. Bar, 10 μm.
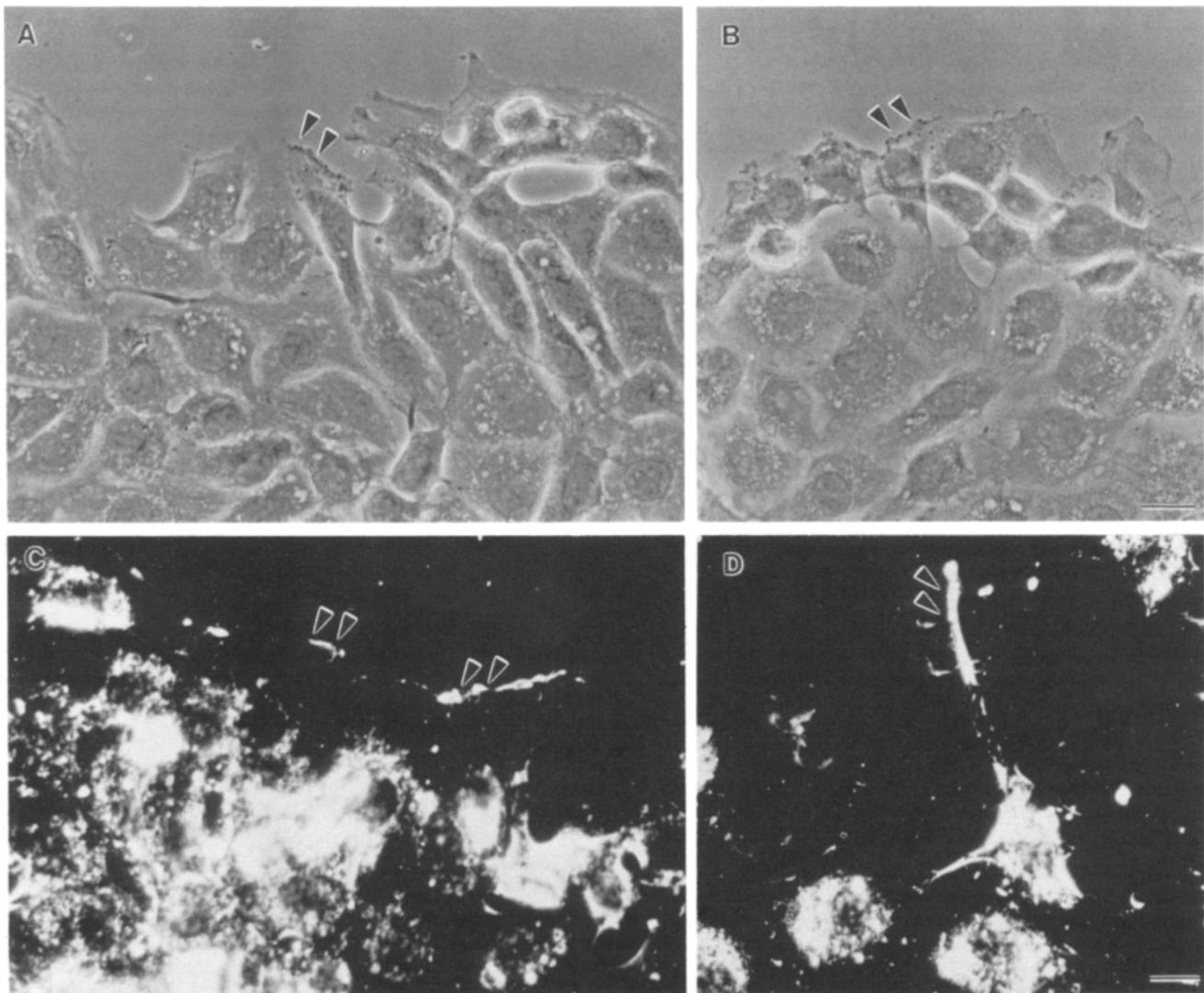
Figure 7. In situ hybridization of actin cDNA-mRNA hybrids. Phase-contrast (*A* and *B*) and dark field images (*C* and *D*) of endothelial monolayers fixed 15 (*A*), 30 (*B*), and 60 min (*C* and *D*) after injury. Phase-contrast and dark field images of these four distinct endothelial monolayers (*A–D*) that were fixed before treatment with radiolabeled actin cDNA autoradiography reveal specific localization over the regions of ruffling membrane (*A* and *C*, *arrows*), pseudopods (*B*, *arrows*), and filopods (*D*, *arrows*) present at the wound edge. The cells away from the would edge do not show this membrane-associated localization pattern although specific hybridization can be detected surrounding each nucleus. Both the nuclear and wound zones are devoid of specific reaction product. Bar, 5 μm.

short, roughly equivalent to the length of a spectrin dimer (Atkinson et al., 1982; Brenner and Korn, 1980; Pinder et al., 1977). It is possible that actin–spectrin interactions contribute to erythrocyte actin filament length. The plasma membrane may also confer limits on actin filament length since filament ends may be captured or effectively "capped" at the membrane (Atkinson et al., 1982; Tsukita et al., 1984). On the other hand, actin interacts with (at least) a ternary complex of binding proteins, including bands 4.1, spectrin, and possibly ankyrin (Bennett, 1985; Brenner and Korn, 1980; Kordelli et al., 1990). Erythrocyte tropomyosin (Fowler and Bennett, 1984), tropomodulin (Fowler, 1987, 1990), and myosin (Fowler et al., 1985; Wong et al., 1985) may also be involved in regulating the extent of actin filament cross-linking and filament length. Clearly, the mechanisms regulating this precisely formatted arrangement of membrane-associated cytoskeletal proteins together with erythrocyte actin are poorly understood.

There may be physical constraints on erythrocyte actin filament length that give rise to its foreshortened length. As has been well studied for the other actins from muscle, there are specific strain limits on the length of flexible polymers, like actin (Aebi et al., 1986). Filaments that elongate past a specific point, tend to break, especially when sheared (Sato et al., 1987). In addition, pertubations in the angles that establish molecular contact within the filament may also alter bonding rules so as to yield a filament with an altered helical lattice, one that would not support filament elongation. These limitations might yield an altered filament backbone, one that might be prone to breakage in the absence of shear. Furthermore, the sites of interaction that exist for the binding of actin with its accessory proteins may also be structured in a way that prevents filament elongation in vivo. This may be the case for tropomyosin, which selectively prevents actin filament disassembly in vitro (Fowler and Bennett, 1984). It has recently been demonstrated that

the assembly of intact myofibrils in the indirect flight muscle of *Drosophila* is severely perturbed when specific alterations in the coding sequence for muscle actin are produced (Fyrberg et al., 1983). Furthermore, other work indicates that mutagenized β actin present in HUT-14T fibroblastic cells assembles poorly into filaments. In this case, a single amino acid substitution from glycine to aspartic acid yielded an actin molecule with an altered electrophoretic mobility, a foreshortened half-life, and a more rapid rate of synthesis when compared to the wild-type actin (Leavitt and Kakunaga, 1980; Leavitt et al., 1982). It is interesting to point out that the erythrocyte β tubulin gene yields a tubulin that polymerizes into a microtubule of altered stability, solubility and length (Murphy, 1988; Murphy and Wallis, 1983).

Sorting of Contractile Protein Isoforms

Mechanisms regulating cytoskeletal protein isoform sorting have not been adequately studied. Whereas injection studies using fluorescent derivatives of muscle actin placed into nonmuscle cells suggest that heterologous isoforms of actin can readily equilibrate throughout the cytoplasmic pool (DeBaisiso et al., 1988; Wang and Taylor, 1979; Wang, 1987), these experimental results do not address how the cell itself selectively positions the individual isoforms that are expressed simultaneously or sequentially (Rubenstein, 1990).

Some controversy exists regarding whether functional sorting of nonmuscle actin isoforms occurs. Antibodies to the γ isoform were prepared and colocalized with the total cellular actin pool, but a direct localization of beta actin was not performed (Otey et al., 1986). As the authors point out, it is possible that the anti-γ actin antibody failed to discriminate γ and β actins because of epitope masking or sharing, in spite of their demonstration of antibody specificity. In the cell types that were tested by Otey and co-workers (1986), there were no stress fibers that displayed a unique staining pattern for gamma vs. beta actins. using our anti-β actin-specific IgG, we have been able to detect specific domains of β actin that occur along the lengths of a specialized set of pericyte stress fibers, i.e., those fibers that associate with the ventral plasma membrane. This uniqueness of actin isoforms located on individual stress fiber subsets is also reflected in our failure to demonstrate that endothelial and 3T3 cells at rest or those recovering from injury contain an abundance of β actin-enriched stress fibers. While the results of our studies strongly suggest that microdomains of β actin are coassembled into longer gamma actin-containing filaments, we also cannot rule out the possibilities that epitope masking accounts for these unique stress fiber staining patterns or that short β actin filaments are annealed within these heterotypic filaments and/or stress fibers.

Unquestionably, sorting of muscle and nonmuscle actins occurs within cells and tissues that simultaneously express these distinct gene products (DeNofrio et al., 1989; Herman and D'Amore, 1985; Skalli et al., 1989). There is also evidence of injury-induced switching of contractile protein isoforms and their respective mRNAs, events that are reversible concomitant with vascular repair (Barja et al., 1986; Gabbiani et al., 1984). It has been suggested that the cytoskeleton, itself, may position contractile protein isoforms via a network of mRNAs that encode for the proteins (Lawrence and Singer; 1986; Lenk et al., 1977; Pramanik et al., 1986). The earlier work, taken together with our current studies using the β

actin-specific antibodies and radiolabeled cDNAs, suggests that asymmetric placement of mRNAs encoding this contractile protein may, indeed, represent a viable sorting mechanism.

β Actin in Nonerythroid Cells

It is of extreme interest that β actin is selectively positioned against the plasma membrane of the nonerythroid cells tested. In the pericyte as well as the endothelial and 3T3 cells, the concentration of β actin along the cytoplasmic face appears to be locally high (Table I). Earlier studies using gold-labeled actin antibodies in conjunction with transmission electron microscopy revealed that endothelial cells migrating after injury contained a subset of actin filaments that were densely packed against the membrane and were roughly 100–150 nm long (Herman, 1987). While a critical analysis of the actin isoform content of this region was not performed, results of the current studies are suggestive that the filaments may be solely comprised of β actin. The earlier work also revealed that myosin II is excluded from this "terminal web" associated with the membrane. The expression and position of non-erythroid myosin I, which has been demonstrated to preferentially associate with membrane lipids (Adams and Pollard, 1989; Collins and Boysenko, 1984; Hayden et al., 1990), has not been studied in endothelial cells recovering from injury. Nonerythroid spectrin has been characterized and mapped within injured endothelial cells (Pratt et al., 1984), but a preferential association within the motile zone of cytoplasm was not demonstrated. Isoforms of nonerythroid ankyrin have more recently been characterized (Kordelli et al., 1990). The position of ankyrin as well as its isoform may be important in the sorting of β actin in nonerythroid cells. Clearly, more work is required to determine whether β actin-specific binding proteins cooperate during these and other sorting processes.

References

Adams, R. J., and T. D. Pollard. 1989. Binding of myosin I to membrane lipids. *Nature (Lond.).* 340:565–588.

Aebi, U., R. Milloning, H. Salvo, and A. Engel. 1986. The three-dimensional structure of the actin filament revisited. *Ann. NY Acad. Sci.* 483:100–119.

Antonelli-Orlidge, A., K. B. Saunders, S. R. Smith, and P. A. D'Amore. 1989. An activated from of TGF-beta is produced by co-cultures of endothelial cells and pericytes. *Proc. Natl. Acad. Sci. USA.* 86:4544–4548.

Atkinson, M. A. L., J. S. Morow, and V. T. Marchesi. 1982. The polymeric state of actin in the human erythrocyte cytoskeleton. *J. Cell. Biochem.* 18:493–505.

Bandman, E. 1985. Myosin isozyme transitions during muscle development, maturation and disease. *Int. Rev. Cytol.* 9:97–131.

Barja, F., C. Coughlin, D. Berlin, and G. Gabbiani. 1986. Actin isoform synthesis and mRNA levels in quiescent and proliferating rat aortic smooth muscle cells in vivo and in vitro. *Lab. Invest.* 55:226–233.

Bennett, V. 1985. The membrane skeleton of human erythrocytes and its impli-
cations for more complex cells. *Annu. Rev. Biochem.* 54:273–304.

Brenner, S. L., and E. D. Korn. 1980. Spectrin/actin complex isolated from
sheep erythrocytes accelerates actin polymerization by simple nucleation. *J.
Biol. Chem.* 255:1670–1676.

Buchanan, R. A., and R. C. Wagner. 1990. Associations between pericytes and
capillary endothelium in the eel rete mirabile. *Microvasc. Res.* 39:60–76.

Buckingham, M. E. 1985. Actin and myosin multigene families: their expres-
sion during the formation of skeletal muscle. *Essays Biochem.* 20:77–109.

Chamley-Campbell, J. H., G. R. Campbell, and R. Ross. 1979. The smooth
muscle cell in culture. *Physiol. Rev.* 59:1–61.

Chirgwin, J. M., A. E. Przybyla, R. J. MacDonald, and W. J. Rutter. 1979.
Isolation of biologically active ribonucleic acid from sources enriched in
ribonuclease. *Biochemistry.* 18:5194–5199.

Cohen, C. M., and S. F. Foley. 1982. The role of band 4.1 in the association
of actin with erythrocyte membranes. *Biochim. Biophys. Acta.* 688:691–
701.

Collins, J. H., and C. M. Borysenko. 1984. The 110,000 Dalton actin and cal-
modulin-binding protein from intestinal brush border is a myosin-like ATP-
ase. *J. Biol. Chem.* 259:14128–14135.

Craig, S. W., and J. V. Pardo. 1983. Gamma actin, spectrin and intermediate
filament proteins colocalize with vinculin at costameres, myofibril-to-
sarcolemma attachment sites. *Cell Motil.* 3:449–462.

Das, A., R. N. Frank, M. L. Weber, A. Kennedy, C. A. Ridy, and M. Mancini.
1988. ATP causes retinal pericytes to contract in vitro. *Exp. Eye Res.*
46:349–362.

DeBiasio, R. L., Y.-L. Wang, G. W. Fisher, and D. L. Taylor. 1988. The dy-
namic distribution of fluorescent analogues of actin and myosin in protru-
sions at the leading edge of migrating Swiss 3T3 fibroblasts. *J. Cell Biol.*
107:2631–2645.

DeNofrio, D., T. C. Hoock, and I. M. Herman. 1989. Functional sorting of
actin isoforms in microvascular pericytes. *J. Cell Biol.* 109:191–202.

Fallon, J. R., and V. T. Nachmias. 1980. Localization of cytoplasmic and skele-
tal myosins in developing muscle cells by double-label immunofluorescence.
J. Cell Biol. 87:237–247.

Fowler, V. M. 1987. Identification and purification of a novel Mr 43,000
tropomyosin-binding protein from human erythrocyte membranes. *J. Biol.
Chem.* 262:12792–12800.

Fowler, V. M. 1990. Tropomodulin: a cytoskeletal protein that binds to the end
of the erythrocyte tropomyosin and inhibits tropomyosin binding to actin.
J. Cell Biol. 111:471–482.

Fowler, V. M., and V. Bennett. 1984. Erythrocyte membrane tropomyosin:
purification and properties. *J. Biol. Chem.* 259:5978–5989.

Fowler, V. M., J. P. Davis, and V. Bennett. 1985. Human erythrocyte myosin.
Identification and purification. *J. Cell Biol.* 100:47–55.

Fyrberg, E. A., J. W. Mahaffey, B. J. Bond, and N. Davidson. 1983. Tran-
scripts of the six *Drosophila* actin genes accumulate in a stage and tissue
specific manner. *Cell.* 33:115–123.

Gabbiani, G., E. Schmid, S. Winter, C. Chapponier, C. DeChastonay, J. Van-
dekerckhove, K. Weber, and W. W. Franke. 1982. Vascular smooth muscle
cells differ from other smooth muscle cells: predominance of vimentin fila-
ments and a specific alpha actin. *Proc. Natl. Acad. Sci. USA.* 78:298–302.

Gabbiani, G., O. Kocher, W. S. Bloom, J. Vandekerckhove, and K. Weber.
1984. Actin expression in smooth muscle cells of rat aortic intimal thicken-
ing, human atheromatous plaque, and cultured rat aortic media. *J. Clin. In-
vest.* 73:148–152.

Gadasi, H., and E. D. Korn. 1980. Evidence for differential localization of
Acanthamoeba myosin isozymes. *Nature (Lond.).* 286:452–455.

Hayden, S. M., J. S. Wolenski, and M. S. Mooseker. 1990. Binding of brush
border myosin I to phospholipid vesicles. *J. Cell Biol.* 111:443–452.

Herman, I. M. 1987. Extracellular matrix-cytoskeletal interactions in vascular
cells. *Tissue & Cell.* 19:1–19.

Herman, I. M. 1988. Developing probes and methods for morphologic and bio-
chemical analyses of cytoskeletal elements in vascular cells. *CRC Crit. Rev.
Anat. Sci.* 1:133–148.

Herman, I. M., and J. J. Castellot, Jr. 1987. Regulation of smooth muscle
growth by endothelial-synthesized matrices. *Arteriosclerosis.* 7:463–469.

Herman, I. M., and P. A. D'Amore. 1985. Microvascular pericytes contain
muscle and nonmuscle actins. *J. Cell Biol.* 101:43–52.

Herman, I. M., and S. Jacobson. 1988. *In situ* analysis of microvascular peri-
cytes in hypertensive rat brains. *Tissue & Cell.* 20:1–12.

Herman, I. M., P. M. Newcomb, J. E. Coughlin, and S. Jacobson. 1987. Char-
acterization of microvascular cultures from normotensive and hypertensive
rat brains: pericyte-endothelial cell interactions *in vitro*. *Tissue & Cell.*
19:197–206.

Joyce, N. C., M. F. Haire, and G. E. Palade. 1985. Contractile proteins in peri-
cytes. I. Immunoperoxidase localization of tropomyosin. II. Immunocyto-
chemical evidence for the presence of two isomyosins in graded concentra-
tions. *J. Cell Biol.* 100:1379–1395.

Kelley, C., P. A. D'Amore, H. Hechtman, and D. Shepro. 1987. Microvascular
pericyte contractility in vitro: comparison with other cells of the vascular
wall. *J. Cell Biol.* 104:483–490.

Kordeli, E., J. Davis, B. Trapp, and V. Bennett. 1990. An isoform of ankyrin
is localized at nodes of ranvier in myelinated axons of central and peripheral

nerves. *J. Cell Biol.* 110:1341–1352.

Lawrence, J. B., and R. H. Singer. 1986. Intracellular localization of mes-
senger RNAs for cytoskeletal proteins. *Cell.* 45:407–415.

Leavitt, J., and T. Kakunaga. 1980. Expression of a variant form of actin and
additional polypeptide changes following chemical induced in vitro neoplas-
tic transformation of human fibroblasts. *J. Biol. Chem.* 255:1650–1661.

Leavitt, J., G. Bushar, T. Kanunaga, H. Hamada, T. Hirakawa, D. Goldman,
and C. Merril. 1982. Variations in expression of mutant beta actin accom-
panying incremental increases in human fibroblast tumorigenicity. *Cell.*
28:259–268.

Lenk, R., L. Ransom, Y, Kaufman, and S. Penman. 1977. A cytoskeletal struc-
ture with associated polyribosomes obtained from HeLa cells. *Cell.*
10:67–78.

Lin, J.-J.-C., T. E. Hegman, and J. L.-C. Lin. 1988. Differential localization
of tropomyosin isoforms in cultured nonmuscle cells. *J. Cell Biol.*
107:563–572.

Maniatis, T. E., F. Fritsch, and J. Sambrook. 1982. Molecular Cloning: A Lab-
oratory Manual. Cold Spring Harbor Laboratory, Cold Spring Harbor, New
York. 545 pp.

McHugh, K. M., and J. L. Lessard. 1988. The nucleotide sequence of a rat
vascular smooth muscle alpha- actin cDNA. *Nucleic Acid. Res.* 16:4167–
4169.

Murphy, D. B. 1988. Tubulin subunit sorting: analysis of the mechanisms in-
volved in the segregation of unique tubulin isoforms within copolymers. *Pro-
toplasma (Berl.).* 145:176–181.

Murphy, D. B., and K. T. Wallis. 1983. Brain and erythrocyte microtubules
from chicken contain different B-tubulin polypeptides. *J. Biol. Chem.*
258:8357–8364.

Noden, D. M. 1989. Embryonic origins and assembly of blood vessels. *Am.
Rev. Respir. Dis.* 140:1097–1103.

Olmsted, J. B. 1981. Affinity purification of antibodies from diazotized paper
blots of heterogeneous protein samples. *J. Biol. Chem.* 256:11955–11957.

Orlidge, A., and P. A. D'Amore. 1987. Inhibition of capillary endothelial cell
growth by pericytes and smooth muscle cells. *J. Cell Biol.* 105:1455–1462.

Otey, C. A., M. H. Kalnoski, J. L. Lessard, and J. C. Bulinski. 1986. Im-
munolocalization of the gamma isoform of nonmuscle actin in cultured cells.
J. Cell Biol. 102:1726–1737.

Owens, G. K., A. Loeb, D. Gordon, and M. M. Thompson. 1986. Expression
of smooth muscle specific alpha-isoactin in cultured vascular smooth muscle
cells: relationship between growth and cytodifferentiation. *J. Cell Biol.*
102:343–352.

Pardo, J. F., M. F. Pittenger, and S. W. Craig. 1983. Subcellular sorting of
isoactins: selective association of gamma actin with skeletal muscle mito-
chondria. *Cell.* 32:1093–1103.

Pinder, J. C., and W. Gratzer. 1983. Structural and dynamic states of actin in
the erythrocyte. *J. Cell Biol.* 96:768–775.

Pinder, J. C., D. Bray, and W. B. Gratzer. 1977. Control of interaction of spec-
trin and actin by phosphorylation. *Nature (Lond.).* 270:752–754.

Pramanik, S. K., R. W. Walsh, and J. Bag. 1986. Association of messenger
RNA with the cytoskeletal framework in rat L6 myogenic cells, *Eur. J. Bio-
chem.* 160:221–230.

Pratt, B. M., A. S. Harris, J. S. Morrow, and J. A. Madri. 1984. Mechanisms
of cytoskeletal regulation: modulation of endothelial cell spectrin by the ex-
tracellular matrix. *Am. J. Pathol.* 117:349–354.

Rovner, A. S., R. A. Murphy, and G. K. Owens. 1986. Expression of smooth
muscle and nonmuscle myosin heavy chains in cultured vascular smooth
muscle cells. *J. Biol. Chem.* 261:14740–14745.

Rubenstein, P. A. 1990. Functional importance of multiple actin isoforms. *Bio-
essays.* 12:309–315.

Sato, M:, W. H. Schwartz, and T. D. Pollard. 1987. Dependence of the me-
chanical properties of actin/alpha actinin gels on deformation rate. *Nature
(Lond.).* 325:828–830.

Schwartz, R. J., and K. N. Rothblum. 1981. Gene switching in myogenesis:
differential expression of the actin multigene family. *Biochem. J.* 20:4122–
4129.

Skalli, O., M.-F. Pelte, M.-C. Peclet, G. Gabbiani, P. Gugliotta, G. Bussolati,
M. Ravazzola, and L. Orci. 1989. Alpha smooth muscle actin, a differentia-
tion marker of smooth muscle cells, is present in microfilamentous bundles
of pericytes. *J. Histochem. Cytochem.* 37:315–321.

Tsukita, S., S. Tsukita, and H. Ishikawa. 1984. Bidirectional polymerization
of G-actin on the human erythrocyte membrane. *J. Cell Biol.* 98:1102–1110.

Wang, Y.-L. 1987. Mobility of filamentous actin in living cytoplasm. *J. Cell
Biol.* 105:2811–2816.

Wang, Y.-L., and D. L. Taylor. 1979. Distribution of fluorescently labeled ac-
tin in living sea urchin eggs during development. *J. Cell Biol.* 82:672–679.

Warembourg, M., O. Tranchant, M. Atger, and E. Milgrom. 1986.
Uteroglobin mRNA: localization in rabbit uterus and lung by *in situ* hybrid-
ization. *Endocrinology.* 119:1632–1640.

Wong, A. J., D. P. Kiehart, and T. D. Pollard. 1985. Myosin from human
erythrocytes. *J. Biol. Chem.* 260:46–49.

Yost, J. C., and I. M. Herman. 1990. Substratum-induced stress fiber assembly
in vascular endothelial cells during spreading *in vitro*. *J. Cell Sci.*
95:507–20.